Journal of Organometallic Chemistry, 435 (1992) 55–72
Elsevier Sequoia S.A., Lausanne
JOM 22684

Early-transition-metal ketene complexes: synthesis, reactivity and structure of ketene complexes of bis(trimethylsilyl)niobocene, X-ray structure of [Nb(η^5-$C_5H_4SiMe_3$)$_2$Br(Ph_2C=C=O–*C*,*O*)

Antonio Antiñolo and Antonio Otero

Departamento de Química Inorgánica, Orgánica y Bioquímica, Facultad de Químicas, Universidad de Castilla-La Mancha, Paseo de la Universidad 4, 13071 Ciudad Real (Spain)

Mariano Fajardo [a], Carmen Lopez-Mardomingo [b]

[a] *Departamento de Química Inorgánica and* [b] *Departamento de Química Orgánica, Campus Universitario, Universidad de Alcalá de Henares, 28871 Alcalá de Henares (Spain)*

Dominique Lucas, Yves Mugnier

Laboratoire de Synthèse et d'Electrosynthèse Organométalliques Associé au CNRS (URA 33), Faculté des Sciences, 6 bd. Gabriel, 21000 Dijon (France)

Maurizio Lanfranchi and Maria Angela Pellinghelli

Istituto di Chimica Generale ed Inorganica, Università di Parma, Centro di Studio per la Strutturistica Diffrattometrica del CNR, Viale delle Scienze 78, I-43100 Parma (Italy)

(Received December 12, 1991)

Abstract

The "carbenoid-like" complex [Nb(η^5-$C_5H_4SiMe_3$)$_2$Br] **1a** reacts with 1 equivalent of several ketenes, R_1R_2C=C=O, to give the niobium(V) complexes [Nb(η^5-$C_5H_4SiMe_3$)$_2$Br(R_1R_2C=C=O–*C*,*O*)] (**2a**, $R_1 = R_2 =$ Ph; **3a**, $R_1 = R_2 =$ Me; **4a**, $R_1 =$ Ph, $R_2 =$ Me; **5a**, $R_1 =$ Ph, $R_2 =$ Et) with the expected C=O bonding mode found in several early-transition-metal moieties. The protonation of these complexes with 1 equivalent of H^+ (an ethereal solution of HBF_4) affords the acyl cationic niobocene [Nb(η^5-$C_5H_4SiMe_3$)$_2$Br(R_1R_2HCC=O)]$^+$ (**6a**, $R_1 = R_2 =$ Ph; **7a**, $R_1 = R_2 =$ Me; **8a**, $R_1 =$ Ph, $R_2 =$ Me; **9a**, $R_1 =$ Ph, $R_2 =$ Et).

The ketene complexes **2a** and [Nb(η^5-$C_5H_4SiMe_3$)$_2$Cl(R_1R_2C=C=O–*C*,*O*)] **2b** (hereafter **b** refers to the chloro-complexes) undergo a two-electron reduction without transformation of the ketene moiety to give the same anionic niobium(III) species [Nb(η^5-$C_5H_4SiMe_3$)$_2$(η^2-(C,O)R_1R_2C=C=O)]$^-$ **10** by an ECE process. The structure of **2a** was determined by X-ray diffraction methods. The crystals are

---

Correspondence to: Professor A. Otero, Departamento de Química Inorgánica, Orgánica y Bioquímica, Facultad de Químicas, Universidad de Castilla-La Mancha, Paseo de la Universidad 4, 13071 Ciudad Real, Spain.

triclinic, space group $P\bar{1}$ with $Z = 4$ in a unit cell of dimensions $a = 16.063(7)$, $b = 19.108(8)$, $c = 10.696(6)$ Å, $\alpha = 99.89(2)$, $\beta = 94.64(2)$, $\gamma = 111.95(2)°$. The structure was solved from diffractometer data by Patterson and Fourier methods and refined by blocked full-matrix least-squares on the basis of 9706 observed reflections, to R and R_w values of 0.0391 and 0.0567 respectively. The diphenylketene and the two Cp′ rings (Cp′ = $C_5H_4SiMe_3$) are η^2(C–O) and η^5 respectively. The niobium atom is also bonded to a Br atom. If the centroids of the Cp′ rings and the midpoint of the C–O ketene bond are considered, the Nb atom displays a distorted tetrahedral coordination.

Introduction

In recent years the usefulness of organometallic compounds as reagents in fine organic synthesis has increased considerably [1]. The changes induced in the reactivity of molecules widely used in organic synthesis are important to develop new selective synthetic pathways. Ketenes, ketenimines, and related heterocumulenes are very reactive organic molecules whose organic chemistry is now well defined, and several reviews on aspects of the synthesis and reactivity are available [2].

Ketenes can model the coordination mode and activation of CO_2 by transition metal complexes [3]. Furthermore, transition metal ketene complexes have been proposed as intermediates in the Fischer–Tropsch conversion of synthesis gas (CO/H_2) to hydrocarbons [4].

Ketene complexes have been prepared by several indirect procedures, such as carbonylation of carbene complexes and deprotonation of acyl complexes. In only a few cases have early-transition-metal ketene complexes been prepared directly by coordination of free ketenes, probably owing to the instability of ketene complexes under the reaction conditions [5].

Ketene ligands are known to bind to transition-metal centres, ML_n, in two principal fashions, via side-on bonding of C=C or C=O, as in **A** and **B** respectively:

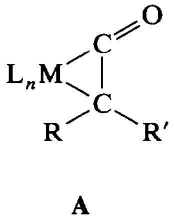

A

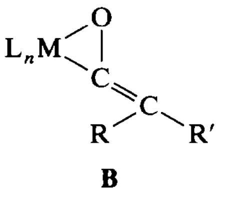

B

The η^2(C–C) mode **A** has been observed for late transition metals, and the η^2(C–O) mode **B** for early transition metals [5]. Indeed, model extended Hückel calculation [6] suggests that a supplemental oxygen lone pair → d donation in the η^2(C–O) mode is especially favourable for electron-poor metals, and this strong donor interaction would favour the η^2(C–O) coordination mode in early-transition-metal complexes.

In our research with bis(trimethylsilyl)niobocene complexes, we have found that the 16-electron complexes [$Nb(\eta^5\text{-}C_5H_4SiMe_3)_2X$] (X = Cl or Br) are excellent precursors for activating heterocumulenes such as isocyanates [7] and ketenimines [8]. We have continued to develop the chemistry of these niobium(III) compounds and here we report the results of our studies of the preparation and structure of η^2(C–O) ketene niobocene complexes. Their reactivity toward the reducing agent sodium amalgam and HBF_4 acid is described. Electrochemical data are also discussed, together with the molecular and crystal structure of an η^2(C–O) ketene complex.

Results and discussion

Synthesis and properties

Recently we have developed the chemistry of niobocene complexes, and we have found that trimethylsilyl-substituted cyclopentadienyl rings are particularly useful in modifying the reactivity of these complexes [9]. Three years ago we published [7a] a simple method for the preparation of an air-sensitive 16-electron niobium(III) complex $[Nb(\eta^5\text{-}C_5H_4SiMe_3)_2Cl]$ **1b** in high yield. This turns out to be an excellent reagent to activate heterocumulenes such as isocyanates, isothiocyanates and carbodiimide. These promising results prompted us to explore metal-promoted reactions with other heterocumulenes. In fact, ketene and ketenimine ligands react in a similar fashion with complex **1b** to give the desired ketenimine [8] and ketene [10] complexes. In the course of our work with ketene ligands Halfon *et al.* [11] published analogous results with **1b**. We have prepared the complexes $[Nb(\eta^5\text{-}C_5H_4SiMe_3)_2Cl(R_1R_2C{=}C{=}O\text{-}C,O)]$ (**2b**, $R_1 = R_2 =$ Ph; **3b**, $R_1 = R_2 =$ Me; **4b**, $R_1 =$ Ph, $R_2 =$ Me; **5b**, $R_1 =$ Ph, $R_2 =$ Et) as yellow crystalline solids which exhibit the spectral (IR, ^{1}H and ^{13}C NMR) data described [10,11].

In an attempt to extend the field of ketene niobocene complexes to carry out a complete chemical and electrochemical reduction study, we have prepared bromoketene complexes (eq. 1) in high yields (*ca.* 85%)

$$\left[Nb(\eta^5\text{-}C_5H_4SiMe_3)_2Br\right] + R_1R_2C{=}C{=}O \longrightarrow \left[Nb(\eta^5\text{-}C_5H_4SiMe_3)_2Br(R_1R_2C{=}C{=}O\text{-}C,O)\right] \quad (1)$$

2a, $R_1 = R_2 =$ Ph; **3a**, $R_1 = R_2 =$ Me; **4a**, $R_1 =$ Ph, $R_2 =$ Me; **5a**, $R_1 =$ Ph, $R_2 =$ Et.

All these complexes were air stable microcrystalline yellow solids. They are very soluble in THF and aromatic hydrocarbons and less soluble in alkanes. All the ketene niobium(V) complexes are diamagnetic. They have been characterized by standard analytical methods.

IR, ^{1}H and ^{13}C NMR data are particularly useful. The IR spectra of free ketenes show a strong band at *ca.* 2100 cm^{-1} corresponding to their carbonyl vibrations. In our complexes the ν(C=C=O) band of the ketene moiety appears between 1580 and 1701 cm^{-1} and this value agrees with the bathochromic shift reported for other bonded ketene complexes [5,10,11] with a η^2(C,O) coordination. It has been pointed out that the value ν(C=C=O) in the η^2-(C,C) coordination mode ketene complexes appears at higher energies than in the η^2(C,O) coordination mode, principally because the oxygen atom is bound to the metal in the latter. In addition, the X-ray crystal structure determined for **2a** has confirmed the expected η^2(C–O) coordination mode. The ^{1}H NMR spectra show the resonances corresponding to both the cyclopentadienyl rings and the ketene ligand. However, the most useful spectroscopic data for determining the ketene bonding mode are the ^{13}C NMR resonances [12]. In our complexes the ketene C^1 coordinated to the niobium atom shows a resonance at a downfield chemical shift typical of metal acyls [13] in the range 157.1–173.7 ppm, whereas the C^2 shows a resonance between 85.8 and 105.4 ppm in à range characteristic of sp^2 carbon atoms [13]:

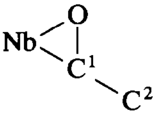

The ^1H and ^{13}C NMR data indicate the presence of only one isomer of the *exo* and *endo* possibilities:

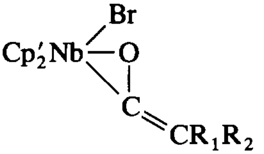

exo

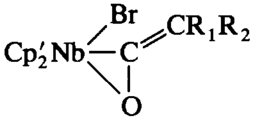

endo

The X-ray crystal structure shows that crystalline **2a** has the favoured *exo*-structure. Similar behaviour has been observed [8] in ketenimine complexes.

With an unsymmetrical ketene, an isomeric mixture due to *E–Z* isomerism about the C=C bond is detected by ^1H NMR spectroscopy:

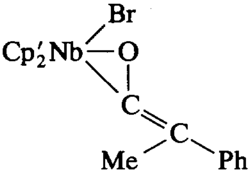

exo-E

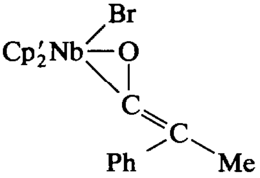

exo-Z

Probably the more stable isomer is the E and for **4a** and **5a** the *E*–Z ratios are 67:33 and 85:15 respectively. Attempts to change the *E–Z* ratio by heating the NMR tube solution were unsuccessful. The relatively few studies of ketene complexes indicate that these ligands have high reactivity to nucleophilic and electrophilic attack. Bruno *et al.* [14] have described electrophilic attack of H^+ on the coordinated ketene in niobocene complexes, affording the first niobocene acyl derivatives, $[Nb(\eta^5\text{-}C_5H_4SiMe_3)_2Cl(R_1R_2HCC{=}O)]^+$. We have carried out reactions with H^+ on the bromo (ketene) derivatives and we have found similar behaviour (eq. 2);

$$[Nb(\eta^5\text{-}C_5H_4SiMe_3)_2Br(R_1R_2C{=}C{=}O)] + HBF_4 \longrightarrow [Nb(\eta^5\text{-}C_5H_4SiMe_3)_2Br(R_1R_2HCC{=}O)]BF_4 \quad (2)$$

6a, $R_1 = R_2 = Ph$; **7a**, $R_1 = R_2 = Me$; **8a**, $R_1 = Ph$, $R_2 = Me$; **9a**, $R_1 = Ph$, $R_2 = Et$.

Complexes **6a–9a** were isolated as white solids in diethyl ether, indefinitely stable under an inert atmosphere. The IR spectra show the acyl $\nu(C{=}O)$ between 1630 and 1612 cm^{-1}. The ^1H NMR spectra show resonances corresponding both to cyclopentadienyl rings and to the acyl ligand. The ^{13}C NMR spectra provide useful information about the structure of the acyl complexes. In our complexes, the C^1 (acyl carbon) resonates downfield at *ca.* 280–289 ppm, similar to the data previously reported by Erker and Rosenfeldt [15] for acyl zirconocene complexes.

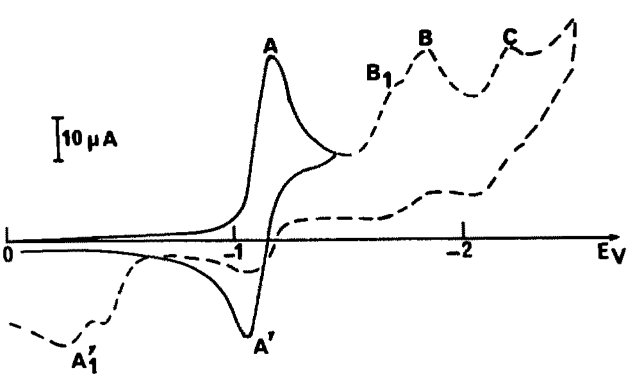

Fig. 1. Cyclic voltammograms of [Nb(η^5-$C_5H_4SiMe_3$)$_2$$Cl_2$]: ———, alone; ------, in the presence of $Ph_2C{=}C{=}O$. Sweep rate 0.2 V s^{-1}, starting potential 0 V.

C^2 shows a resonance at *ca.* 45–63 ppm, in a range characteristic of sp^3 carbon atoms [13]:

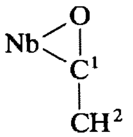

Electrochemical studies

We have previously described the electrochemical behaviour of ketenimine niobocene complexes [8]. Now we describe studies on **2a** and **2b**. In THF at a platinum electrode, the cyclic voltammogram of [Nb(η^5-$C_5H_4SiMe_3$)$_2$$Cl_2$] exhibits a system of reversible peaks, A/A′. However in the presence of $Ph_2C{=}C{=}O$, three new reduction peaks, B_1, B, and C, appear in the voltammogram. On the reverse scan, the oxidation peak A′ is weak and a new oxidation peak A'_1 is found at lower cathodic potential (Fig. 1).

Electrolysis of the dichloride complex in the presence of an excess of the ketene carried out at −1.4 V, corresponding to the plateau of wave A, consumes almost 2 equivalents of electrons. In the polarography of the electrolysed solution, reduction B and oxidation A'_1 waves appear. If the solution is stored under argon the reduction wave A corresponding to the reduction of the dichloride complex is observed.

The number of electrons consumed in the electrolysis is dependent both on the concentration of the ketene and the working conditions. The most important point is that the isolation of **2b** is not possible by electrochemical synthesis. This is probably due to the reduction of the initially electrogenerated **2b** by the anionic niobium(III) complex that remains in the solution. In fact, we have observed that the addition of the ketene to the electrogenerated solution of [Nb(η^5-$C_5H_4SiMe_3$)$_2$$Cl_2$]$^-$ produces the complex [Nb(η^5-$C_5H_4SiMe_3$)$_2$$Cl_2$].

We have also studied the electrochemical behaviour of **2a** and **2b**. Their polarograms show a reduction wave, B* and B respectively, situated at −1.65 and -1.73 V.

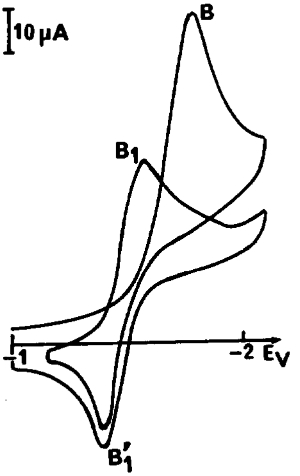

Fig. 2. Cyclic voltammogram of **2b** in THF. Sweep rate 0.2 V s^{-1}, starting potential −1.0 V.

In cyclic voltammetry the corresponding peaks are observed. Reversing the potential scan produces an oxidation peak B_1' [16*]. In the second scan a new reduction peak B_1 situated at a lower cathodic potential is observed (Figs. 2 and 3). The waves B_1–B_1' show all the characteristics of a reversible system and we have found the same values for the potential of B_1 and B_1' in both **2a** and **2b**. No modification of the cyclic voltammogram was observed after the addition of ethanol as a proton source. When the electrolysis of **2b** is carried out at −1.5 V, corresponding to the plateau of wave B, the polarogram of the electrolysed solution after the consumption of 1.2 equivalents of electrons shows the B_1 and C reduction waves together with an ill defined oxidation wave A'_1. The EPR spec-

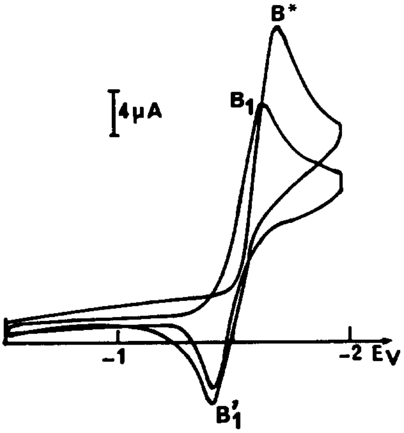

Fig. 3. Cyclic voltammogram of **2a** in THF. Sweep rate 0.1 V s^{-1}, starting potential −0.5 V.

---

* Reference number with asterisk denotes a note in the list of references.

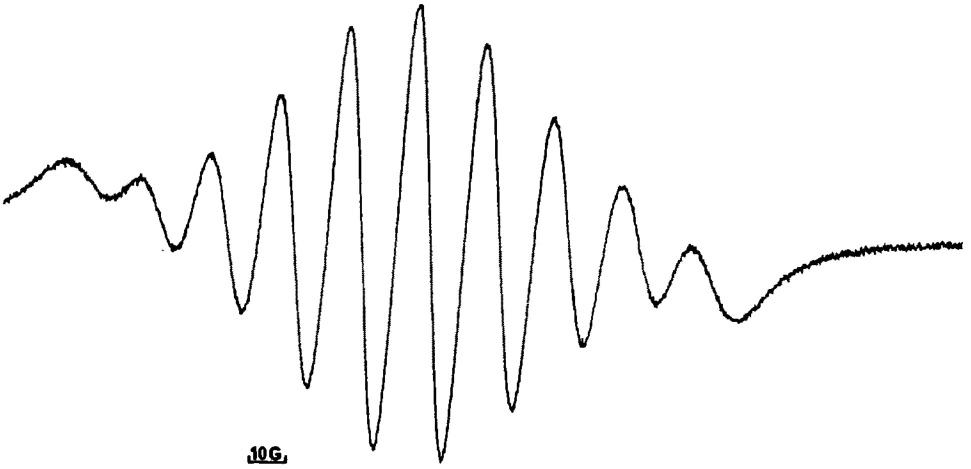

Fig. 4. ESR spectrum of the electrolysed solution of **2b** at −1.5 V and consumption of 1.2 F.

trum of this solution shows a characteristic ten-line signal for a Nb^{IV} ($I = 9/2$) paramagnetic complex ($g = 1.9966$, $A_{Nb} = 18.08$ g) (Fig. 4).

After an exhaustive electrolysis of **2b** at the potential of the plateau of wave B, two electrons are consumed and the polarogram shows the oxidation wave B_1' (Fig. 6(b)). In cyclic voltammetry, the reversible system B_1–B_1' is observed (Fig. 5). After 30 min under argon we observed that the wave B_1' disappears and the reduction wave C appears (Fig. 6(c)). When the electrolysis is carried out in the presence of ethanol, after two-electron reduction, wave C is observed. When the electrolysis of **2a** is carried out at the potential corresponding to the plateau of wave B^*, the polarogram of the electrolysed brown solution shows the oxidation wave B_1'. After

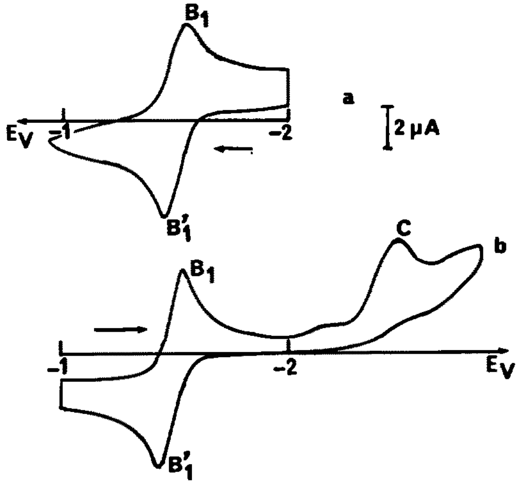

Fig. 5. Cyclic voltammogram of the electrolysed solution of **2b** after two-electron reduction. Sweep rate 0.2 V s^{-1}, starting potential (a) −2 V and (b) −1 V.

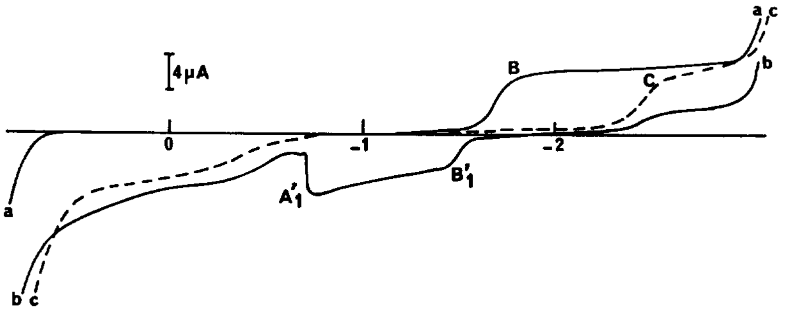

Fig. 6. Polarogram (average current) of **2b** in THF: (a) before electrolysis; (b) after two-electron reduction at −1.5 V; (c) after 30 min at room temperature.

reoxidation at the potential of the plateau of wave B'_1 the reduction waves B_1 and C appear. The same reversible system, B_1–B'_1, and the EPR spectrum described above for **2b** were found. These results can be rationalized by Scheme 1.

The two-electron reduction of **2a** and **2b** (peaks B* and B respectively) affords the anionic niobium(III) complex **10** by an ECE process. The first step yields an anionic 19-electron species which is very unstable and undergoes loss of halide to give, in each case the paramagnetic niobium(IV) complex $[Nb(\eta^5\text{-}C_5H_4SiMe_3)_2(R_1R_2C{=}C{=}O\text{-}C,O)]$ **11**. Complex **11** is immediately reduced to give complex **10** (peak B_1). The formation, during the electrolysis of **2a** or **2b**, of complex **11**, whose EPR spectrum has been recorded, can be explained by an outer-sphere electron transfer reaction between **2a** or **2b** and **10** since the potential difference is 140 mV. Compound **10** generated at the electrode diffuses towards the bulk of the solution and meets **2a** or **2b** which diffuse towards the electrode

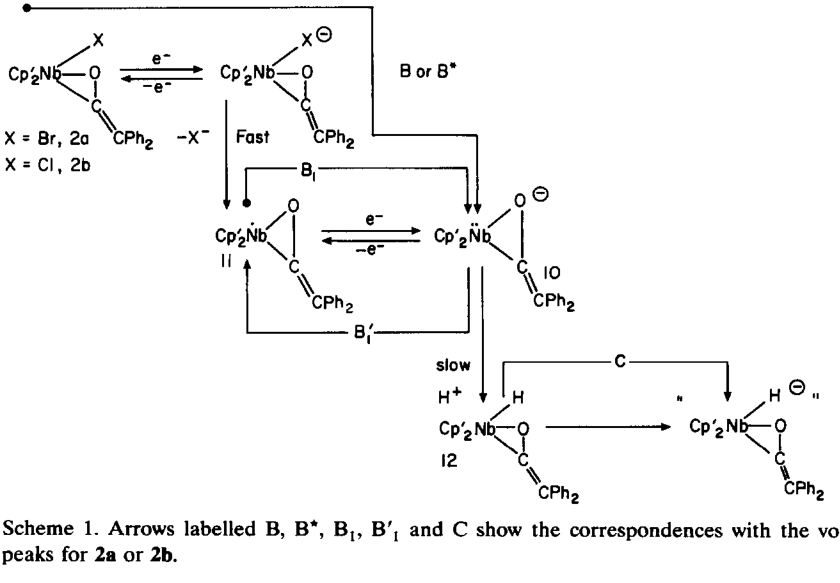

Scheme 1. Arrows labelled B, B*, B_1, B'_1 and C show the correspondences with the voltammogram peaks for **2a** or **2b**.

and the reaction (eq. 3) takes place. Similar behaviour has been observed in ketenimine complexes [8].

$$\underset{\mathbf{2a,\,2b}}{[\mathrm{Nb}(\eta^5\text{-}C_5H_4SiMe_3)_2X(Ph_2C{=}C{=}O)]} + \underset{\mathbf{10}}{[\mathrm{Nb}(\eta^5\text{-}C_5H_4SiMe_3)_2(Ph_2C{=}C{=}O)]^-} \longrightarrow \underset{\mathbf{11}}{2[\mathrm{Nb}(\eta^5\text{-}C_5H_4SiMe_3)_2(Ph_2C{=}C{=}O)]} + X^- \qquad (3)$$

When reduction of **2a** and **2b** is carried out complex **10** is quantitatively generated. This can be oxidized at the potential of the peak B_1' to give **11**. Complex **10** is a relatively stable product and it undergoes a slow protonation (from adventitious protons) to give the hydride complex $[\mathrm{Nb}(\eta^5\text{-}C_5H_4SiMe_3)_2H(\eta^2\text{-}(C,O)Ph_2C{=}C{=}O)]$ **12** [11]. Moreover, **12**, prepared chemically, exhibits the reduction wave C [17*]. In an attempt to isolate complex **11** we investigated the reaction of **2a** or **2b** with sodium amalgam. The reaction with 1 equivalent of Na–Hg leads to a mixture (1 : 1) of complex **12** and starting material. We think that the initially obtained complex **11** is immediately reduced, as indicated by the electrochemical data, to give complex **10**, which yields complex **12** as the only product.

In conclusion, our key observation is that the keteneniobocene complexes undergo a two-electron reduction with loss of chloride, but without change in the ketene moiety. Similar electrochemical behaviour has been found in ketenimine [8] and carbon disulphide [18] niobocene complexes. Halfon *et al.* [11] have published the voltammograms for keteneniobocene complexes and have proposed a one-electron reduction *via* a process which involves a structural change in the ketene moiety to give a niobaenolate intermediate. The formation of the hydride complex **12** has also been proposed as the result of a β-H elimination process in a neutral $\mathrm{Nb^{III}}$ acyl intermediate.

Crystal and molecular structure of $[\mathrm{Nb}(\eta^5\text{-}C_5H_4SiMe_3)_2Br\{\eta^2\text{-}(C,O)Ph_2C{=}C{=}O\}]$ *(2a)*

The unit cell of **2a** contains two crystallographically independent, but essentially identical, molecules. The structure of one of them is depicted in Fig. 7, together with the atom-numbering scheme; the most important bond distances and angles are given in Table 1.

The complex consists of a diphenylketene ligand η^2(C–O) bonded to the $\mathrm{NbCp'_2Br}$ unit ($\mathrm{Cp'} = C_5H_4SiMe_3$) adopting an *exo* isomerism. If the CE(2) and CE(3) ring centroids and the midpoint of the C(1)–O(1) bond are considered as coordination sites, the coordination geometry around niobium can be considered as a distorted tetrahedron, the fourth coordination site being occupied by the bromine atom. This geometry is very similar to that observed for $[\mathrm{ZrCp^*_2(Py)}\{\eta^2\text{-}(C,O)H_2C{=}CO\}]$ (**A**) [19], $[\mathrm{ZrCp_2(CH_3)}\{\eta^2\text{-}(C,O)H_2C{=}CO\}]\mathrm{Na}\cdot 2\mathrm{THF}$ (**B**) [20], and for the niobocene acyl compound $[\mathrm{NbCp'_2Cl}\{\eta^2\text{-}(C,O)EtPhHCCO\}]^+$ (**C**) [14]. The largest coordination angle obviously involves the two Cp′ rings (CE(2)–Nb–CE(3) = 128.9(2)° [129.9(2)°], (hereafter the value in brackets refers to the second independent molecule). The rather small Br–Nb–O(1) angle (77.4(1)° [79.0(1)°]) is notable, but similar values have been found independently of the nature and of the steric hindrance of the fourth coordination ligand (Cl, Me, Py) in **A** ($\mathrm{N_{Py}}$–Zr–O =

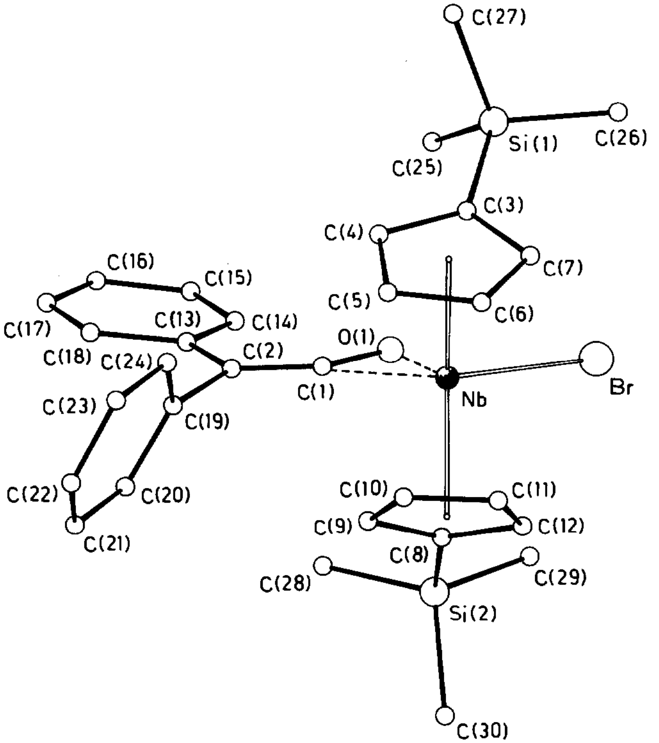

Fig. 7. View of the molecular structure of $[Nb(\eta^5\text{-}C_5H_4SiMe_3)_2Br(Ph_2C{=}C{=}O\text{-}C,O)]$ **2a** with the atom-numbering scheme.

76.77(5)°), in **B** (C_{Me}–Zr–O = 78.4(4)°), in **C** (Cl–Zr–O = 80.9(1)°), and greater values in the dinuclear zirconocene phosphine functionalized ketene complexes $[(ZrCp_2Cl)_2(\mu\text{-}Ph_2PHC{=}CO)]$ [21] (Cl–Zr–O = 83.2(2)°) and $[(ZrCp_2Cl)_2(\mu\text{-}Me_2PHC{=}CO)]$ [22] (Cl–Zr–O = 84.0(3)°). The two Cp′ rings are η^5-bonded to the niobium atom, but the Nb–C bonds are not quite equal (minimum and maximum values 2.413(4), 2.489(3) and 2.395(3), 2.453(3) Å [2.399(4), 2.473(3) and 2.409(3), 2.451(3) Å]) and this suggests that the ring carbon atoms interact with the metal in a slightly asymmetric way. The cyclopentadienyl rings are planar with the Si(1) and Si(2) atoms deviating from the mean plane through them by 0.341(2), 0.366(3) Å [0.278(2), 0.311(2) Å], pushed away from the Nb atom. The relative orientation of the Cp′ rings in both complexes is intermediate between the eclipsed and the staggered ($\tau_{av}[C_{Cp'}$–CE(2)–CE(3)–$C_{Cp'}]$ = 17.3(4)° [15.3(4)°]), and that of the $SiMe_3$ is "*cis*" while another rotational isomer was found in the niobocene acyl complex **C**. The O(1)C(1)C(2)C(13)C(19)NbBr moiety, almost planar (max. dev. for C(19) = 0.244(4) Å [0.237(4) Å]), bisects roughly the CE(2)–Nb–CE(3) angle.

The Nb–O(1) bond distance (2.082(2) Å [2.085(2) Å]) is significantly shorter than the Nb–O bond (2.233(4) Å) found in the niobocene acyl compound **C** while the Nb–C(1) bond length (2.145(3) Å [2.132(3) Å]) is similar (2.121(5) Å). The C–O bond distance (1.303(4) Å [1.298(4) Å]) falls in the range for a η^2(C–O) bonded ketene (1.282(9)–1.339(9) Å) [19,20,23] and is out of the range (1.311(4)–1.413(7)

Table 1

Important interatomic distances (Å) and angles (deg) for **2a**

Bond distances	*Molecule 1*	*Molecule 2*
Nb–Br	2.647(1)	2.654(1)
Nb–O(1)	2.082(2)	2.085(2)
Nb–C(1)	2.145(3)	2.132(3)
Nb–CE(1)	2.011(2)	2.006(3)
Nb–CE(2)	2.134(3)	2.123(4)
Nb–CE(3)	2.111(3)	2.111(3)
O(1)–C(1)	1.303(4)	1.298(4)
C(1)–C(2)	1.351(5)	1.346(5)
C(2)–C(13)	1.471(3)	1.481(4)
C(2)–C(19)	1.490(5)	1.500(5)
C(3)–C(4)	1.417(6)	1.421(5)
C(4)–C(5)	1.411(4)	1.409(4)
C(5)–C(6)	1.404(6)	1.406(6)
C(6)–C(7)	1.394(5)	1.395(6)
C(3)–C(7)	1.439(4)	1.429(4)
C(8)–C(9)	1.421(5)	1.430(5)
C(9)–C(10)	1.413(4)	1.405(5)
C(10)–C(11)	1.402(5)	1.388(6)
C(11)–C(12)	1.402(5)	1.388(6)
C(8)–C(12)	1.414(4)	1.433(5)
Si(1)–C(3)	1.885(3)	1.890(3)
Si(2)–C(8)	1.874(3)	1.869(4)
Bond angles		
Br–Nb–O(1)	77.4(1)	79.0(1)
Br–Nb–C(1)	113.1(1)	114.8(2)
O(1)–Nb–C(1)	35.9(1)	35.8(1)
Br–Nb–CE(1)	95.5(1)	97.1(2)
Br–Nb–CE(2)	104.2(2)	103.0(2)
O(1)–Nb–CE(2)	112.4(2)	110.9(2)
C(1)–Nb–CE(2)	105.6(2)	103.6(2)
CE(1)–Nb–CE(2)	109.9(2)	108.1(2)
CE(2)–Nb–CE(3)	128.9(2)	129.9(2)
Br–Nb–CE(3)	103.8(2)	104.1(2)
O(1)–Nb–CE(3)	114.9(2)	115.1(2)
C(1)–Nb–CE(3)	101.4(2)	102.1(2)
CE(1)–Nb–CE(3)	108.9(2)	109.4(2)
Nb–O(1)–C(1)	74.7(2)	74.0(2)
O(1)–C(1)–C(2)	133.2(3)	133.8(4)
Nb–C(1)–O(1)	69.4(2)	70.1(2)
Nb–C(1)–C(2)	156.9(3)	156.0(3)
C(1)–C(2)–C(13)	121.9(4)	122.9(4)
C(1)–C(2)–C(19)	117.9(3)	118.6(4)
C(13)–C(2)–C(19)	120.0(3)	118.5(3)

Estimated standard deviations are given in parentheses. CE(1), CE(2), CE(3) are the midpoint of the O(1)–C(1) bond, and the centroids of the C(3)...C(7) and C(8)...C(12) rings respectively.

Å) for a μ–η^2(C–O) ketene complex [21,22,24]. The shortening of the C–O bond with respect to the enol C–O single bond (unweighted sample mean $d = 1.333$ Å) [25] indicates a partial retention of double bond character. The lengthening of the C=C bond (1.351(5) Å [1.346(5) Å]) is normal for η^2(C–O) bonded RPhC=C=O ketenes (R = Me, Ph) [23]. The value of the O(1)–C(1)–C(2) angle (133.2(3)° [133.8(4)°]) is due to steric hindrance and electronic effects. The largest values are observed for the trigonal complexes (135.9(5) [23a], 136.5(6)° [23b]) and the smallest ones for $H_2C{=}C{=}O$ ketene tetrahedral complexes (124.1(8) [20], 126.3(2)° [19]).

The phenyl group (C(13)–C(18)) is tilted with respect to the O(1)C(1)C(2)C(13) C(19) moiety by 16.6(1)° [8.1(1)°] and this small value allows electron delocalization over the O(1)C(1)C(2)C(13) system. In fact the C(2)–C(13) bond distance (1.471(3) Å [1,481(4) Å]) is shorter than the other $C{-}C_{Ph}$ bond length (C(2)–C(19) = 1.490(5) Å [1.500(5) Å]). The approximate coplanarity of one phenyl ring involves the formation of a rather strong intramolecular hydrogen bond (C(14)...O(1) = 2.899(4) Å [2.947(4) Å], H(14)...O(1) = 2.21 Å [2.26 Å]) and a significant enlargement of the C(1)–C(2)–C(13) bond angle (121.9(4)° [122.9(4)°]) found also in other phenyl or diphenylketene complexes [23,24a]. The intramolecular hydrogen bond could explain the greater stability of the *exo-E* isomer with respect to the *exo-Z* isomer. Also, in **A** the ketene oxygen is involved in a $C_{Py}{-}H...O$ hydrogen bond, forming a five-membered ring instead of a six-membered ring.

Conclusion

We report in this paper new η^2(C–O) ketene niobocene complexes prepared by direct coordination of ketene, and also the acyl cationic complexes arising from protonations. We have found, by electrochemical studies, that the ketene complexes undergo two-electron reductions which do not affect the ketene moiety. Studies of the reactivity both of ketene and of acyl niobocene complexes are currently in progress.

Experimental

Syntheses and physical measurements

All reactions were performed using standard Schlenk techniques under an atmosphere of dry, oxygen-free, nitrogen or argon. Solvents were distilled from appropriate drying agents and degassed before use. Elemental analyses were performed with a Perkin–Elmer 240B microanalyser. NMR spectra were recorded on a Varian FT 80A instrument. Chemical shifts are reported (δ) from $SiMe_4$. IR spectra were recorded as Nujol mulls between CsI plates in the region 4000–200 cm^{-1} with a Perkin–Elmer PE883 IR spectrometer. In the electrochemical experiments, a saturated calomel reference electrode, separated from the solution by a sintered glass disk, was used. The auxiliary electrode was of platinum wire. In all cases the supporting electrolyte was tetrabutylammonium hexafluorophosphate (0.2 M); the salt (Fluka) was dried and deoxygenated before use. A Tacussel UAP4 unit connected to a Tektronix oscilloscope (linear potential sweep experiments), a three-electrode Tacussel Tipol polarograph, an Amel 552 potentiostat and a Tacussel IG 5 integrator were used.

$[Nb(\eta^5\text{-}C_5H_4SiMe_3)_2X]$ (X = Cl or Br) and ketenes were prepared according to the published methods [7,26].

*$[Nb(\eta^5\text{-}C_5H_4SiMe_3)_2Br(\eta^2\text{-}(C,O)R_1R_2C{=}C{=}O)]$ [$R_1 = R_2 = Ph$ **2a**; $R_1 = R_2 = Me$ **3a**; $R_1 = Ph$, $R_2 = Me$ **4a**; $R_1 = Ph$, $R_2 = Et$ **5a**].* To a solution of [Nb(η^5-

$C_5H_4SiMe_3)_2Br]$ (500 mg, 1.12 mmol) in 50 ml of hexane or pentane was added a solution of diphenylketene (2 mmol) in hexane. The mixture was stirred for 2 h at room temperature. The solution became increasingly yellow and a yellow precipitate was formed. After 3 h at −15°C, the solution was filtered and the remaining solid was recrystallized from hot ethanol to give **2a**. Derivatives **3a–5a**, were obtained by similar procedures.

2a: IR (Nujol): ν(C=C=O) 1580 cm^{-1}. ^1H NMR (C_6D_6): δ 0.25 (s, 18 H, $SiMe_3$), 4.52 (2 H), 4.76 (2 H), 6.11 (2 H), 6.48 (2 H) (each a complex signal, C_5H_4), 7.28–8.00 (mc, 10 H, $O{=}C{=}CPh_2$); $^{13}C\{^1H\}$ NMR (THF) δ 0.28 ($SiMe_3$), 119.0 (C^1), 103.9, 104.5, 123.8, 126.0 (C^2, C^3, C^4, C^5; exact assignment not possible), 105.4 ($Ph_2C{=}C{=}O$), 173.7 ($C{=}C{=}O$), 143.5, 144.1 (C_{ipso} of phenyl groups), 120.3, 127.5, 128.8, 129.6, 129.8, 132.7 (C of phenyl groups). Anal. Found (calc. for $C_{30}H_{36}BrNbOSi_2$): C, 56.03 (56.09); H, 5.60 (5.65).

3a: IR (Nujol): ν(C=C=O) 1701 cm^{-1}. ^1H NMR ($CDCl_3$): δ 0.23 (s, 18H, $SiMe_3$), 5.36 (2 H), 5.85 (2 H), 6.34 (2 H), 6.62 (2 H) (each a complex signal, C_5H_4), 1.84 (s, 3H), 1.90 (s, 3H) ($C{=}C(CH_3)_2$). $^{13}C\{^1H\}$ NMR ($CDCl_3$): δ −1.10 ($SiMe_3$), 114.1 (C^1), 99.7, 105.2, 117.9, 127.7 (C^2, C^3, C^4, C^5; exact assignment not possible), 85.8 ($Me_2C{=}C{=}O$), 157.1 ($C{=}C{=}O$), 19.6, 21.5 ($={CMe_2}$). Anal. Found (calc. for $C_{20}H_{32}BrNbOSi_2$): C, 46.25 (46.35); H, 6.31 (6.22).

4a: IR (Nujol): ν(C=C=O) 1632 cm^{-1}. ^1H NMR ($CDCl_3$; **4a** (E isomer)): δ 0.18 (s, 18H, $SiMe_3$), 4.58 (2 H), 4.97 (2 H), 5.50 (2 H), 6.29 (2 H) (each a complex signal, C_5H_4), 2.05 (s, 3H, CH_3), 7.28–7.57 (mc, 5 H, Ph); ($CDCl_3$; **4a** (Z isomer)): δ 0.29 (s, 18H, $SiMe_3$), 4.62 (2 H), 5.31 (2 H), 5.80 (2 H), 6.60 (2 H) (each a complex signal, C_5H_4), 2.12 (s, 3H, CH_3), 7.28–7.57 (mc, 5 H, Ph). Anal. Found (calc. for $C_{25}H_{34}BrNbOSi_2$): C, 51.53 (51.74); H, 5.99 (5.90).

5a: IR (Nujol): ν(C=C=O) 1622 cm^{-1}. ^1H NMR ($CDCl_3$; **5a** (E isomer)): δ 0.16 (s, 18H, $SiMe_3$), 5.47 (2 H), 5.86 (2 H), 6.43 (2 H), 6.62 (2 H) (each a complex signal, C_5H_4), 1.37 (t, 3H, $J = 7$ Hz, $CH_2{-}CH_3$), 2.63 (c, 2H, $J = 7$ Hz, $CH_2{-}CH_3$), 7.28–7.71 (mc, 5 H, Ph); ($CDCl_3$; **5a** (Z isomer)): δ 0.21 (s, 18H, $SiMe_3$), 5.52 (2 H), 5.94 (2 H), 6.13 (2 H), 6.57 (2 H) (each a complex signal, C_5H_4), 1.13 (t, 3H, $J = 8$ Hz, $CH_2{-}CH_3$), 2.86 (c, 2H, $J = 8$ Hz, $CH_2{-}CH_3$), 7.28–7.71 (mc, 5 H, Ph). Anal. Found (calc. for $C_{26}H_{36}BrNbOSi_2$): C, 52.17 (52.54); H, 6.00 (6.10).

*$[Nb(\eta^5\text{-}C_5H_4SiMe_3)_2Br(\eta^2\text{-}(C,O)R_1R_2HC{-}C{=}O)]BF_4$ [$R_1 = R_2 = Ph$ **6a**; $R_1 = R_2 = Me$ **7a**; $R_1 = Ph$, $R_2 = Me$ **8a**; $R_1 = Ph$, $R_2 = Et$ **9a**].* To a diethyl ether suspension of **2a** (500 mg, 0.68 mmol) $HBF_4 \cdot Et_2O$ (0.68 mmol) was added causing bleaching of the yellow colour. After 5 min at room temperature a colourless solid precipitate was formed which was isolated by filtration. It was crystallized from dichloromethane–hexane and identified as complex **6a**. Derivatives **7a–9a** were obtained by identical procedures.

6a: IR (Nujol): ν(C=O) 1630 cm^{-1}. ^1H NMR ($CDCl_3$): δ 0.34 (s, 18H, $SiMe_3$), 6.43 (2 H), 6.56 (2 H), 6.79 (2 H), 6.94 (2 H) (each a complex signal, C_5H_4), 7.65–8.13 (mc, 10 H, $O{=}C{=}CPh_2$). $^{13}C\{^1H\}$ NMR ($CDCl_3$): δ 0.90 ($SiMe_3$), 125.3 (C^1), 106.8, 108.3, 124.3, 126.6 (C^2, C^3, C^4, C^5; exact assignment not possible), 63.5 ($Ph_2HC{-}C{=}O$), 289.3 ($C{=}C{=}O$), 139.2, 140.3 (C_{ipso} of phenyl groups), 126.3, 131.4, 132.7, 133.6, 133.8, 136.2 (C of phenyl groups). Anal. Found (calc. for $C_{30}H_{37}BBrF_4NbOSi_2$): C, 49.50 (49.40); H, 5.01 (4.97).

7a: IR (Nujol): ν(C=O) 1612 cm^{-1}. ^1H NMR ($CDCl_3$): δ 0.27 (s, 18H, $SiMe_3$), 1.68 (d, 6H, $J = 5$ Hz $CH(CH_3)_2$), 4.01 (mc, 1H, $CH(CH_3)_2$), 6.41 (2 H), 6.48 (2

H), 6.57 (2 H), 6.87 (2 H) (each a complex signal, $C_5\mathit{H}_4$). $^{13}C\{^1H\}$ NMR ($CDCl_3$): δ −0.48 (Si*Me*$_3$), 122.6 (C^1), 106.0, 109.8, 119.2, 127.1 (C^2, C^3, C^4, C^5; exact assignment not possible), 45.1 ($(CH_3)_2HC$–C=O), 286.0 (C–*C*=O), 19.9 ($CH(\mathit{C}H_3)_2$). Anal. Found (calc. for $C_{20}H_{33}BBrF_4NbOSi_2$): C, 39.81 (39.69); H, 5.40 (5.33).

8a: IR (Nujol): ν(C=O) 1616 cm^{-1}. ^1H NMR ($CDCl_3$): δ 0.30 (s, 18H, Si*Me*$_3$), 1.86 (d, 3H, *J* = 6.8 Hz, $CH(C\mathit{H}_3)Ph$), 6.50 (c, 1H, J = 6.8 Hz, $C\mathit{H}(CH_3)Ph$) 5.77 (2 H), 6.01 (2 H), 6.59 (2 H), 6.83 (2 H) (each a complex signal, $C_5\mathit{H}_4$), 7.38–7.73 (mc, 5H, *Ph*). $^{13}C\{^1H\}$ NMR ($CDCl_3$): δ −0.04 (Si*Me*$_3$), 123.8 (C^1), 106.5, 111.1, 122.5, 128.4 (C^2, C^3, C^4, C^5; exact assignment not possible), 53.8 ($\mathit{C}H(CH_3)Ph$), 280.2 (C–*C*=O), 21.1 ($CH(\mathit{C}H_3)Ph$), 137.1 (C_{ipso} of phenyl group) 128.4, 129.5, 130.6 (*C* of phenyl group). Anal. Found (calc. for $C_{25}H_{35}BBrF_4NbOSi_2$): C, 45.11 (45.00); H, 5.22 (5.13).

9a: IR (Nujol): ν(C=O) 1612 cm^{-1}. ^1H NMR ($CDCl_3$): δ 0.33 (s, 18H, Si*Me*$_3$), 2.24 (mc, 5H, $CH(C\mathit{H}_2C\mathit{H}_3)Ph$), 6.20 (t, 1H, $C\mathit{H}(CH_2CH_3)Ph$) 5.75 (2 H), 6.06 (2 H), 6.51 (2 H), 6.61 (2 H) (each a complex signal, C_5H_4), 7.25–7.74 (mc, 5H, *Ph*). $^{13}C\{^1H\}$ NMR ($CDCl_3$): δ −0.95 (Si*Me*$_3$), 119.4 (C^1), 105.7, 119.3, 120.4, 121.8 (C^2, C^3, C^4, C^5; exact assignment not possible), 59.2 ($\mathit{C}H(CH_2CH_3)Ph$), 281.8 (C–*C*=O) 11.1 (CH_2–$\mathit{C}H_3$), 27.6 ($\mathit{C}H_2$–CH_3), 133.7 (C_{ipso} of phenyl group), 126.7, 128.8, 129.4 (*C* of phenyl group). Anal. Found (calc. for $C_{26}H_{37}BBrF_4NbOSi_2$): C, 45.12 (45.83); H, 5.30 (5.32).

X-Ray analysis

The crystallographic data for $[Nb(\eta^5\text{-}C_5H_4SiMe_3)_2Br(Ph_2C{=}C{=}O\text{-}C,O)]$ (**2a**) are summarized in Table 2. Unit cell parameters were determined from the Θ values of 30 carefully centred reflections, having $24° < \Theta < 40°$. The reduced cell

Table 2

Experimental data for the X-ray diffraction study of **2a**

Molecular formula	$C_{30}H_{36}BrNbOSi_2$	Crystal dimension (mm)	0.13×0.10×0.42
Molecular weight	641.60	Linear absorption (cm^{-1})	59.257
Crystal system	triclinic	Diffractometer	Siemens AED
Space group	$P\bar{1}$	Scan type	Θ-2Θ
Radiation	Ni-filtered Cu-K_α	Scan speed (Θ min^{-1})	4–12
	($\bar{\lambda}$ = 1.541838 Å)	Scan width	$(\Theta - 0.60)-$ $(\Theta + 0.60 + 0.142 \tan \Theta)$
a (Å)	16.063(7)	2Θ range (deg)	6–140
b (Å)	19.108(8)	Reflections measured	$\pm h$, $\pm k$, l
c (Å)	10.696(6)	Standard reflection	one measured after 50 reflections
α (deg)	99.89(2)	Unique total data	11261
β (deg)	94.64(2)	Unique observed data $[I \geq 2\sigma(I)]$	9706
γ (deg)	111.95(2)	Number of variables	641
V (Å^3)	2962(3)	*R*	0.0391
Z	4	R_w	0.0567
D_{calc} (g cm^{-3})	1.439		
F(000)	1312		

Table 3

Atomic coordinates ($\times 10^4$) and isotropic thermal parameters ($\text{Å}^2 \times 10^4$) with e.s.d.s in parentheses for the non-hydrogen atoms of **2a**

	x	y	z	U^a
Molecule 1				
Nb(1)	2026(1)	4959(1)	406(1)	393(1)
Br(1)	1164(1)	5877(1)	1039(1)	591(1)
Si(11)	2809(1)	6806(1)	−1165(1)	542(1)
Si(21)	1677(1)	4788(1)	3983(1)	602(4)
O(11)	3003(1)	5880(1)	1753(2)	468(7)
C(11)	3361(2)	5372(2)	1498(3)	434(10)
C(21)	4139(2)	5332(2)	1994(3)	450(9)
C(31)	2453(2)	5737(2)	−1260(3)	480(10)
C(41)	3034(2)	5336(2)	−1189(3)	512(12)
C(51)	2508(2)	4533(2)	−1558(3)	557(14)
C(61)	1600(3)	4422(2)	−1915(3)	599(12)
C(71)	1553(2)	5146(2)	−1691(3)	539(12)
C(81)	1521(2)	4373(2)	2219(3)	478(11)
C(91)	2042(2)	4001(2)	1596(3)	472(10)
C(101)	1586(2)	3608(2)	338(3)	518(11)
C(111)	770(2)	3714(2)	169(3)	559(12)
C(121)	732(2)	4175(2)	1317(3)	525(12)
C(131)	4816(2)	5963(2)	2990(3)	505(11)
C(141)	4619(2)	6560(2)	3691(3)	599(12)
C(151)	5272(3)	7151(2)	4641(4)	707(15)
C(161)	6139(3)	7176(2)	4871(4)	814(15)
C(171)	6348(3)	6603(3)	4176(4)	769(17)
C(181)	5703(2)	6005(2)	3265(4)	665(16)
C(191)	4256(2)	4592(2)	1597(3)	490(11)
C(201)	4394(2)	4184(2)	2503(4)	630(14)
C(211)	4413(3)	3461(3)	2126(4)	767(21)
C(221)	4319(3)	3133(2)	856(4)	753(18)
C(231)	4205(3)	3523(2)	−69(4)	657(14)
C(241)	4176(2)	4247(2)	319(3)	545(12)
C(251)	3522(3)	7366(2)	400(4)	758(16)
C(261)	1795(3)	7030(2)	−1469(5)	783(19)
C(271)	3482(3)	7018(2)	−2510(4)	797(19)
C(281)	2816(3)	4916(3)	4749(4)	903(25)
C(291)	1566(5)	5728(3)	4323(5)	1227(36)
C(301)	785(4)	4057(4)	4609(5)	1454(33)
Molecule 2				
Nb(2)	3057(1)	186(1)	6713(1)	424(1)
Br(2)	3946(1)	−703(1)	7087(1)	722(2)
Si(12)	2285(1)	−1696(1)	3945(1)	615(4)
Si(22)	3198(1)	314(1)	10416(1)	561(3)
O(12)	2040(1)	−742(1)	7189(2)	498(8)
C(12)	1688(2)	−241(2)	7068(3)	450(10)
C(22)	870(2)	−222(2)	7196(3)	454(10)
C(32)	2677(2)	−613(2)	4504(3)	503(11)
C(42)	2110(2)	−193(2)	4601(3)	500(11)
C(52)	2655(3)	604(2)	4850(3)	598(13)
C(62)	3561(3)	686(2)	4840(3)	660(15)
C(72)	3585(2)	−47(2)	4670(3)	603(12)
C(82)	3452(2)	767(2)	9001(3)	488(11)
C(92)	2957(2)	1144(2)	8418(3)	500(10)
C(102)	3467(2)	1543(2)	7567(3)	588(14)

Table 3 (continued)

	x	y	z	U [a]
Molecule 2				
C(112)	4280(2)	1442(2)	7617(3)	617(12)
C(122)	4289(2)	985(2)	8493(3)	565(12)
C(132)	94(2)	−887(2)	7417(3)	465(9)
C(142)	172(2)	−1557(2)	7648(4)	607(13)
C(152)	−578(3)	−2177(2)	7782(5)	757(16)
C(162)	−1437(3)	−2165(2)	7685(5)	832(17)
C(172)	−1525(2)	−1496(2)	7480(4)	686(15)
C(182)	−781(2)	−869(2)	7342(3)	572(12)
C(192)	753(2)	520(2)	7184(3)	476(11)
C(202)	597(2)	921(2)	8296(4)	586(12)
C(212)	539(3)	1633(2)	8337(4)	722(17)
C(222)	629(3)	1949(2)	7282(5)	815(18)
C(232)	760(3)	1550(2)	6151(4)	748(18)
C(242)	823(2)	842(2)	6113(3)	579(11)
C(252)	1465(4)	−2236(2)	4903(5)	972(25)
C(262)	3272(4)	−1966(3)	3899(5)	987(26)
C(272)	1710(3)	−1904(2)	2261(4)	776(17)
C(282)	1961(3)	−74(2)	10464(4)	735(16)
C(292)	3640(3)	−456(3)	10441(5)	875(25)
C(302)	3826(3)	1134(3)	11820(4)	866(20)

[a] Equivalent isotropic U defined as one-third of the trace of the orthogonalized U_{ij} tensor.

was checked with use of programs TRACER [27] and NEWLAT [28]. Data were collected at room temperature, the individual profiles having been analysed by the method of Lehmann and Larsen [29]. Intensities were corrected for Lorentz and polarization effects; a semi-empirical absorption correction was applied (maximum and minimum values were 1.3626 and 0.7571) [30]. Only the observed reflections were used in the structure solution and refinement. The structure was solved by Patterson and Fourier methods, and refined first by full-matrix least-squares with isotropic thermal parameters, and then by blocked full-matrix least-squares with anisotropic thermal parameters in the last cycles for all non-hydrogen atoms. The hydrogen atoms were placed at their geometrically calculated positions (C–H = 1.00 Å) and refined "riding" on the corresponding carbon atoms. After the final cycles, no parameter shifted by more than 0.58 esd, and the biggest remaining peak in the final difference map was equivalent to about 0.71 eÅ^3. In the final cycles of refinement a weighting scheme, $w = K[\sigma^2(F_o) + g\ F_o^2]^{-1}$, was used; at convergence the K and g values were 1.0000 and 0.0043 respectively, and the goodness of fit was 0.7925. The analytical scattering factors, corrected for the real and imaginary parts of the anomalous dispersions, were taken from ref. 31. All calculations were carried out on the CRAY X-MP/48 computer of the Centro di Calcolo Elettronico Interuniversitario dell'Italia Nord Orientale (CINECA, Casalecchio di Reno, Bologna) and on the GOULD POWERNODE 6040 of the Centro di Studio per la Strutturistica Diffrattometrica del C.N.R., Parma using the SHELX-76 and the SHELXS-86 systems of crystallographic computer programs [32]. The final atomic coordinates for the non-hydrogen atoms are given in Table 3.

A complete list of bond lengths and angles and lists of hydrogen-atom coordinates, thermal parameters and structure factors are available from the authors.

Acknowledgments

We gratefully acknowledge financial support from Dirección General de Investigación Científica y Técnica (DGICYT) (Grant No. PB86-0101) of Spain and Acción Integrada Hispano-Francesa (Grant No HF-106). We thank Dr. Loic Rouiller for the ESR experiments, Mr. Youssef Mourad for his interest and Mrs. Marie Thérèse Compain for her technical assistance.

References and notes

1 J.P. Collman, L.S. Hegedus, J.R. Norton and R.G. Finke, Principles and Applications of Organotransition Metal Chemistry, Part III, University Science Books, Mill Valley, CA, 1987, p. 669.

2 (a) S. Patai, The Chemistry of Ketenes Allenes and Related Compounds, Wiley, New York, 1980; (b) H. Ulrich, Cycloaddition Reactions of Heterocumulenes, Academic Press, New York, 1967.

3 (a) A.D. Englich and T. Herskovitz, J. Am. Chem. Soc., 99 (1977) 1648 and references cited therein; (b) D.J. Darensbourg and R.A. Kudaroski, Adv. Organomet. Chem., 22 (1983) 129; (c) M.E. Vol'pin and I.S. Kolomnikov, Organomet. React., 5 (1975) 313.

4 (a) P.T. Wolczanski and J.E. Bercaw, Acc. Chem. Res., 13 (1980) 121; (b) C. Masters, Adv. Organomet. Chem., 19 (1979) 63. (c) E.L. Muetterties, T.N. Rhodin, A. Band, C.F. Brucker and W.R. Pretzer, Chem. Rev., 79 (1979) 91; (d) C.K. Rofer De Poorter, Chem. Rev., 81 (1981) 447; (e) W.A. Herrmann, Angew. Chem., Int. Ed. Engl., 21 (1982) 117; (f) G. Blyholder and P.H. Emmet, J. Phys. Chem., 64 (1960) 470; (g) M. Ichikawa, K. Sekizawa, K. Shikakura and M. Kawai, J. Mol. Catal., 11 (1981) 167; (h) M. Akita, A. Kondoh, T. Kawahara, T. Takagi and Y. Moro-Oka, Organometallics, 7 (1988) 366.

5 G.L. Geoffroy and S.L. Bassner, Adv. Organomet. Chem., 28 (1988) 1.

6 S. Nakamura and K. Morokuma, Organometallics, 7 (1988) 1904.

7 (a) A. Antiñolo, S. Garcia-Lledó, J. Martinez de Ilarduya and A. Otero, J. Organomet. Chem., 335 (1987) 85; (b) A. Antiñolo, M. Fajardo, F.A. Jalón, C. López-Mardomingo, A. Otero and C. Sanz-Bernabé, J. Organomet. Chem., 369 (1989) 187.

8 A. Antiñolo, M. Fajardo, C. López-Mardomingo, A. Otero, Y. Mourad, Y. Mugnier, J. Sanz-Aparicio and F. Florencio, Organometallics, 9 (1990) 2919.

9 (a) A. Antiñolo, P. Gómez-Sal, J.M. Martinez de Ilarduya, A. Otero, P. Royo, S. Garcia-Blanco and S. Martinez-Carreras, J. Chem. Soc., Dalton Trans., (1987) 975; (b) A. Antiñolo, J.M. Martinez de Ilarduya, A. Otero, P. Royo, A.M. Manotti Lanfredi and A. Tiripicchio, J. Chem. Soc., Dalton Trans., (1988) 2685.

10 A. Otero, A. Antiñolo, M. Fajardo, F. Jalon, C. López-Mardomingo, C. Sanz, F. Florencio and J. Sanz-Aparicio, Proc. XIII Int. Conf. on Organometallic Chemistry, Turin, The International Union of Pure and Applied Chemistry, 1988, p. 188.

11 S.E. Halfon, M.C. Fermin and J.W. Bruno, J. Am. Chem. Soc., 111 (1989) 5490.

12 B.E. Mann and B.F. Taylor, ^{13}C NMR Data for Organometallic Compounds, Academic Press, New York, 1981.

13 R.M. Silverman, G.C. Gassler and J.C. Merill, Spectrometric Identification of Organic Compounds, Wiley, New York, 1981, 4th edn.

14 J.W. Bruno, M.C. Fermin, S.E. Halfon and G.K. Schulte, J. Am. Chem. Soc., 111 (1989) 8738.

15 G. Erker and F. Rosenfeldt, Angew. Chem., Int. Ed. Engl., 17 (1978) 605.

16 At higher cathodic potential another reduction peak, C, is observed.

17 Studies of the mechanism of reduction of **12** are in progress.

18 Y. Mugnier, (1992) unpublished results.

19 E.J. Moore, D.A. Straus, J. Armantrout, B.D. Santarsiero, R.H. Grubbs and J.E. Bercaw, J. Am. Chem. Soc., 105 (1983) 2068.

20 S.C.H. Ho, D.A. Straus, J. Armantrout, W.P. Schaefer and R.H. Grubbs, J. Am. Chem. Soc., 106 (1984) 2210.

21 S.J. Young, H. Hope and N.E. Schore, Organometallics, 3 (1984) 1585.

22 L.M. Engelhardt, G.E. Jacobsen, C.L. Raston and A.H. White, J. Chem. Soc., Chem. Commun., (1984) 220.

23 (a) S. Gambarotta, M. Pasquali, C. Floriani, A. Chiesi Villa and C. Guastini, Inorg. Chem., 20 (1981)

1173; (b) J.M. Galante, J.W. Bruno, P.N. Hazin, K. Folting and J.C. Huffman, Organometallics, 7 (1988) 1066.

24 (a) G. Fachinetti, C. Biran, C. Floriani, A. Chiesi Villa and C. Guastini, Inorg. Chem., 17 (1978) 2995; (b) R. Choukroun, F. Dahan and D. Gervais, J. Organomet. Chem., 266 (1984) C33; (c) R.M. Waymouth, B.D. Santarsiero, R.J. Coots, M.J. Bronikowski and R.H. Grubbs, J. Am. Chem. Soc., 108 (1986) 1427.

25 F.H. Allen, O. Kennard D.G. Watson, L. Brammer, A.G. Orpen and R. Taylor, J. Chem. Soc., Perkin Trans. II, (1987) S1.

26 E.C. Taylor, A. McKillop and G.H. Hawck, Org. Synth., 52 (1968) 36.

27 S.L. Lawton, R.A. Jacobson, TRACER: The Reduced Cell and its Crystallographic Applications, Ames Laboratory. Available from the Clearinghouse for Federal Scientific and Technical Information, National Bureau of Standards, US Department of Commerce, Springfield, VG, 1965.

28 A. Mugnoli, J. Appl. Crystallogr., 18 (1985) 183.

29 M.S. Lehmann and F.K. Larsen, Acta Crystallogr. A, 30 (1974) 580.

30 N. Walker and D. Stuart, Acta Crystallogr. A, 39 (1983) 158. The program ABSORB was used (F. Ugozzoli, Comput. Chem., 11 (1987) 109).

31 International Tables for X-ray Crystallography, Vol. IV, Kynoch Press, Birmingham, 1974.

32 G.M. Sheldrick, SHELX-76 program for crystal structure determination, University of Cambridge, 1976; SHELXS-86 Program for the solution of crystal structures, University of Göttingen, 1986.